J|A|C|S
ARTICLES
Published on Web 08/17/2004

X-ray Crystal Structures of a Benzonorbornenyl Cation and of a Protonated Benzonorbornenol†

Thomas Laube

Contribution from the Cilag AG, Hochstrasse 201-209, CH-8205 Schaffhausen, Switzerland

Received April 22, 2004 ; Revised Manuscript Received June 30, 2004; E-mail: tlaube@cilch.jnj.com

Abstract: The crystal structure of the 9-methylbenzonorbornenyl cation Me-**1**$^+$ shows a relatively strong interaction between the sp^2-hybridized carbon atom C9 and the aromatic ring (C4a−C9 ≡ C8a−C9 = 1.897(10) Å). The anion $Sb_2F_{11}^-$ is refined as rotationally disordered along the Sb···Sb axis. In sharp contrast to the findings about Me-**1**$^+$, the protonated *anti*-benzonorbornenol **5**$^+$ is essentially an oxonium ion with only weak interaction between the C9 bridge and the aromatic ring despite the fact that it is already a positively charged ion, which upon loss of a water molecule is expected to give the parent cation H-**1**$^+$. The hydrogen atoms on the oxonium O atom are involved in strong hydrogen bonds to chlorosulfonate anions and probably partially disordered despite the large estimated pK_a differences between the corresponding acid−base pairs. The experimentally determined cation structures are compared with structures computed by DFT methods. Detailed experimental procedures are given.

The unsubstituted benzonorbornenyl cation with a positively charged carbon atom C9[1] (H-**1**$^+$) has been discussed for the first time by Bartlett et al.[2] in a solvolytic study. Their kinetic data showed that the solvolysis of **2** is faster than that of **3** but slower than that of **4** (X: leaving group) (Chart 1), and they discussed an interaction between the empty 2p orbital at C9 and the π electrons at the aromatic carbon atoms C4a and C8a. This interpretation followed the suggestions published by Winstein et al.[3] in their landmark paper of 1955. Other solvolytic studies have been carried out to support this interaction, e.g., by Tanida et al.[4] and Tsuno and co-workers.[5] The only direct observations of R-**1**$^+$ (R: Me, *p*-*F*-phenyl) by NMR spectroscopy have been reported by the groups of Shin[6] and Volz,[7] but

Chart 1

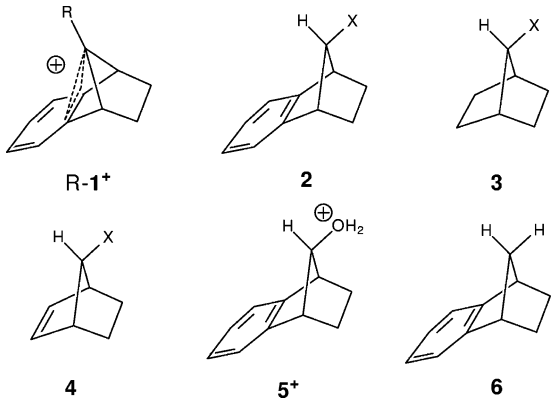

R-**1**$^+$ **2** **3** **4** **5**$^+$ **6**

attempts to observe the unsubstituted H-**1**$^+$ failed due to rapid decomposition on warming up a solution of protonated **2** (X: OH) in superacidic media.[6a] Shin and co-workers assumed that they recorded the NMR spectrum of **5**$^+$ but not of H-**1**$^+$. DFT calculations on H-**1**$^+$ and **6** have been carried out by Houk and co-workers[8] which yielded for H-**1**$^+$ the bond lengths C9−C4a = C9−C8a = 1.980 Å; i.e., they found partial bonds between C9 and the nearest C atoms of the π system. Because the knowledge of the structures of bridged carbocations based on crystal structure analyses is still very limited,[9] we became interested in salts of Me-**1**$^+$ and **5**$^+$, especially because of the useful stability data published by the groups of Shin and Volz.[6a,7]

Results and Discussions

Syntheses and Crystal Growth. The synthesis (Scheme 1) started with the conversion of hexachlorocyclopentadiene (**7**)

† Parts of this work have been presented at the 16th International Conference on Physical Organic Chemistry in San Diego, CA (August 4-9, 2002; abstract LC 3) and at the 9th European Symposium on Organic Reactivity in Oslo, Norway (July 12-17, 2003; abstract OR 42).

(1) Two different numbering schemes for the benzonorbornene system are used. In the older scheme, the atom in the one-carbon bridge has the number 7, whereas, in the newer literature, this atom has the number 9. We use in this paper only the newer numbering scheme.

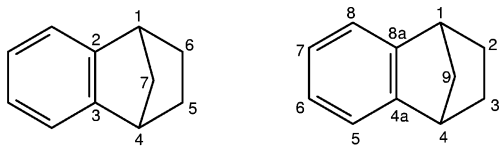

older numbering scheme newer numbering scheme

(2) Bartlett, P. D.; Giddings, W. P. *J. Am. Chem. Soc.* **1960**, *82*, 1240−1246.
(3) Winstein S.; Shatavsky, M.; Norton, C.; Woodward, R. B. *J. Am. Chem. Soc.* **1955**, *77*, 4183−4184.
(4) (a) Tanida, H.; Hata, Y.; Ikegami, S.; Ishitobi, H. *J. Am. Chem. Soc.* **1967**, *89*, 2928−2932. (b) Tanida, H. *Acc. Chem. Res.* **1968**, *1*, 239−245.
(5) Yatsugi, K.; Saeki, Y.; Fujio, M.; Tsuno, Y. *Memoirs of the Faculty of Science, Kyushu University, Ser. C* **1992**, *18*, 223−232; *Chem. Abstr.* **1993**, *118*, 190917.
(6) (a) Lee, C.; Lee, K.; Shin, J.-H. *Chayon Kwahak Taehak Nonmunjip (Soul Taehakkyo)* **1982**, *7*, 51−64; *Chem. Abstr.* **1983**, *98*, 160119. (b) Ahn, Y.-S.; Lee, Y.-N.; Shin, J.-H. *Bull. Korean Chem. Soc.* **1989**, *10*, 481−482. (c) Ryu, G.-Y.; Shin, J.-H. *Bull. Korean Chem. Soc.* **1993**, *14*, 546−548.
(7) Volz, H.; Shin, J.-H.; Miess, R. *J. Chem. Soc., Chem. Commun.* **1993**, 543−544.
(8) Tantillo, D. J.; Hietbrink, B. N.; Merlic, C. A.; Houk, K. N. *J. Am. Chem. Soc.* **2000**, *122*, 7136−7137; **2001**, *123*, 5851.
(9) Laube, T. *Acc. Chem. Res.* **1995**, *28*, 399−405.

10.1021/ja040115t CCC: $27.50

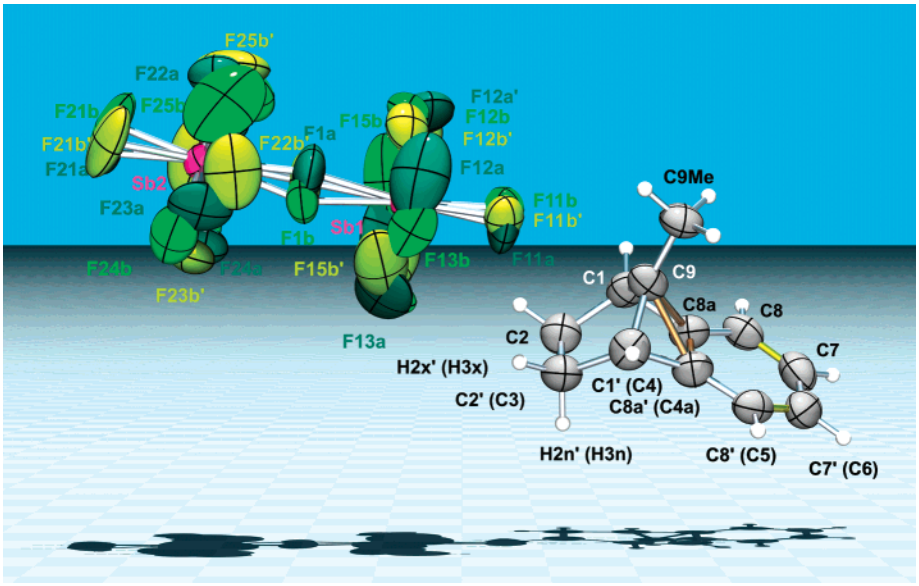

Figure 1. ORTEP representation of the crystal structure of Me-**1**$^+$ $Sb_2F_{11}^-$. The cation and the anion contain a common crystallographic mirror plane passing through C9, C9Me, Sb1, Sb2, F1a, F11a, F21a, F22a, F24a. The symmetry-related atoms have primed labels ($' = x, {}^1/_2 - y, z$), and their chemical names are given in parentheses (the latter ones are used in the discussion). The displacement ellipsoids are drawn at the 50% probability level, and the hydrogen atoms are represented by spheres with a radius of 0.15 Å. The anion site with $m = C_s$ symmetry is drawn with dark green F ellipsoids, and the two anion sites with $1 = C_1$ symmetry (related to each other by the mirror plane) are drawn with light and middle green F ellipsoids. The three center, two electron (3c, 2e) bond is indicated by copper bond sticks, and the shorter bonds of the aromatic[19] ring are drawn as golden bond sticks.

Scheme 1

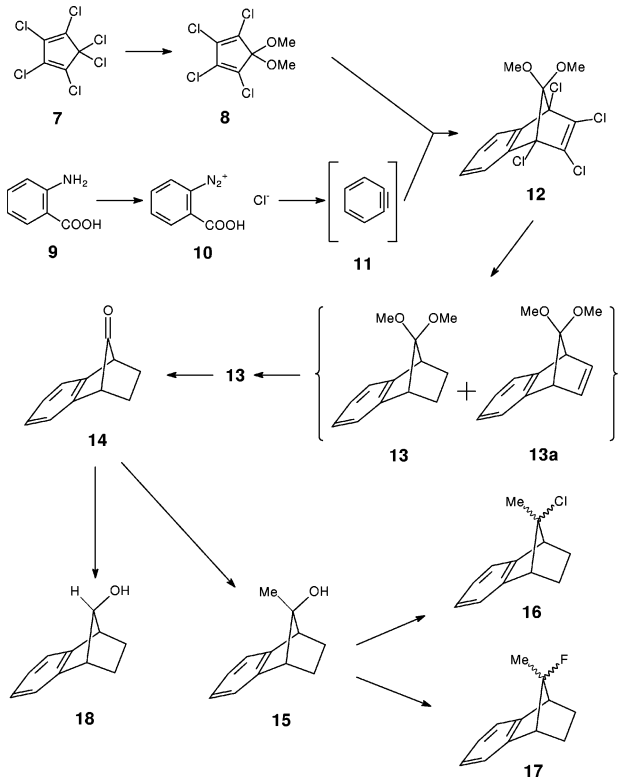

into the dimethylacetal **8**,[10] which was reacted with benzyne (**11**) generated by thermolysis of the diazonium salt **10** of anthranilic acid (**9**).[11] The Diels−Alder adduct **12**[12] was dehalogenated[13] to a mixture of the acetals **13** and **13a**, which were converted into pure **13** by catalytic hydrogenation.[13] Hydrolysis of **13** gave the key intermediate benzonorbornenone (**14**).[14] One part of **14** was converted into the tertiary *anti*-alcohol **15** by a Grignard reaction with MeMgI.[4a] The chloride **16** (one stereoisomer of unknown configuration) was prepared in analogy to 7-methyl-7-norbornyl chloride[15] by reaction with concentrated HCl, the fluoride **17** (one stereoisomer of unknown configuration) in analogy[16] by reaction with HF/pyridine. The secondary alcohol **18** was prepared by reduction of another part of **14** with $LiAlH(OtBu)_3$.[17] The SO_2ClF for the crystal growth experiments was prepared from SO_2Cl_2 and NaF[18] and redistilled. The reaction of **17** with somewhat more than 2 equiv of SbF_5 and subsequent recrystallization from methylene chloride gave crystalline Me-**1**$^+$ $Sb_2F_{11}^-$. Slow addition of a solution of **18** dissolved in methylene chloride to a solution of $ClSO_3H$ in methylene chloride gave upon concentration crystalline **5**$^+$ $SO_3Cl^-\cdot CH_2Cl_2$.

Crystal Structures and DFT Calculations. The structure of Me-**1**$^+$ $Sb_2F_{11}^-$ is shown in Figure 1; see also Tables S1 and S2 (Supporting Information). The cation and the anion both contain a crystallographic mirror plane. The anion is rotationally disordered around the Sb1−Sb2 axis, and the fluorine atoms of the three anion sites and their labels are represented with different shades of green. The cation does not show disorder, although its atomic displacement parameters are relatively large. The most remarkable feature of the structure is the relatively strong bending of the C9 bridge toward the aromatic[19] ring atoms C4a and C8a (C9−C4a ≡ C9−C8a = 1.897(10) Å),

(10) Gassman, P. G.; Marshall, J. L. *Org. Synth.* Coll. Vol. *5*, 424−428.
(11) Dürr, H.; Nickels, H.; Pacala, L. A.; Jones, M., Jr. *J. Org. Chem.* **1980**, *45*, 973−980.
(12) Wilt, J. W.; Vasiliauskas, E. *J. Org. Chem.* **1970**, *35*, 2410−2411.
(13) Ranken, P. F.; Battiste, M. A. *J. Org. Chem.* **1971**, *36*, 1996−1998.
(14) Wilt, J. W.; Vasiliauskas, E. *J. Org. Chem.* **1972**, *37*, 1467−1472.
(15) Lustgarten, R. K.; Lhomme, J.; Winstein, S. *J. Org. Chem.* **1972**, *37*, 1075−1078.
(16) Laube, T. *Helv. Chim. Acta* **1994**, *77*, 943−956.
(17) Okada, K.; Tomita, S.; Oda, M. *Bull. Chem. Soc. Jpn.* **1989**, *62*, 459−468.
(18) Tullock, C. W.; Coffman, D. D. *J. Org. Chem.* **1960**, *25*, 2016−2019.
(19) The term aromatic is still used for Me-**1**$^+$ for simplicity, although a significant perturbation of the π system is observed due to the (3c, 2e) bond which is also indicated by the bond length alternation (see the bond length pattern in **5**$^+$ and **6** in Table S2).

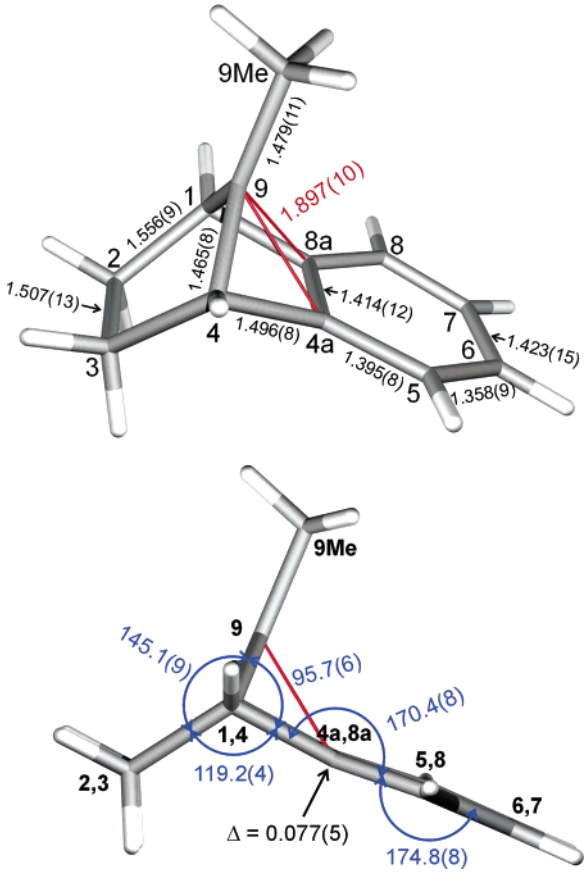

Figure 2. Geometry of the cation in the crystal structure of Me-**1**$^+$ $Sb_2F_{11}^-$ (Distances and pyramidalizations Δ in Å. Blue: interplanar angles in deg. Red: C4a−C9, C8a−C9). Bottom: approximate Newman projection along C1−C4.

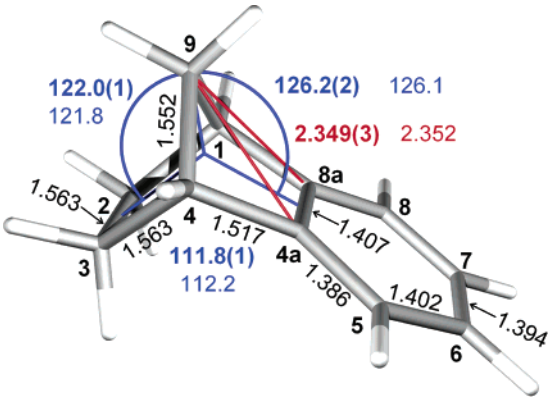

Figure 3. Geometry of benzonorbornene (**6**; distances in Å, angles in deg). Blue: interplanar angles. Red: C4a−C9, C8a−C9. Bold: average from three precise structures with aromatic substituents from the Cambridge file. Plain: computed with B3LYP/6-311+G(d,p).

leading to an angle between the C9 and the C4a/C8a bridge of 95.7(6)°; see Figure 2. This indicates a strong interaction between the two bridges, because the corresponding distances and the corresponding angle in benzonorbornene (as a reference for the absence of such an interaction) are 2.35 Å and 126°; see Figure 3.

The aromatic ring shows bond length alternation: C5−C6 ≡ C7−C8 = 1.358(9) Å are short, C6−C7 = 1.423(15) Å and C4a−C5 ≡ C8−C8a = 1.395(8) Å are longer by 0.065(17) and 0.037(12) Å, respectively. The bond C4a−C8a = 1.414(12) Å is longer by 0.056(15) Å but must be considered as a special

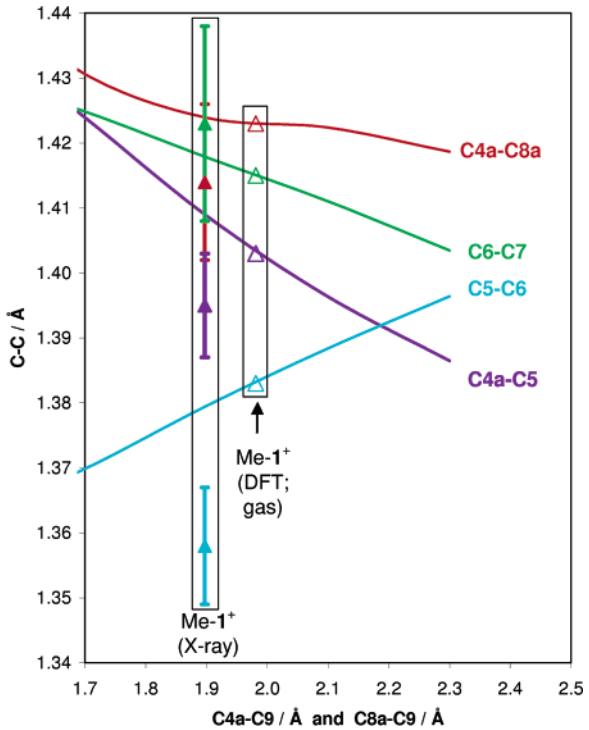

Figure 4. Computed benzene ring C−C bond lengths of Me-**1**$^+$ as functions of the bond length C4a−C9 = C8a−C9. The abscissa can be seen as the reaction coordinate of the approach of the C9 bridge toward the C4a−C8a bond retaining $m = C_s$ symmetry. The structures of the conformations were optimized at the B3LYP/6-311+G(d,p) level with the constraints C4a−C9 = C8a−C9 = 1.5(0.2)2.3 Å (*x*(*y*)*z* means lower bound *x*, increment *y*, upper bound *z*; relaxed potential energy surface scan). The plotted functions are interpolants. The bond lengths from the crystal structure (with error bars) and from the fully optimized structure are drawn as points with the corresponding color (data: see Table S2).

case due to the proximity of the positively charged C9. The bond lengths in the aromatic ring of the computed structure of benzonorbornene (**6**) show a different pattern; see Figure 3 (short: C4a−C5, C6−C7, C8−C8a). The C9−C9Me bond (1.479(11) Å) is slightly shorter than a C_{sp2}-CH_3 bond (average length:[20] 1.503(1) Å), presumably due to C−H hyperconjugation, although the shortening (0.024(11) Å) is not very significant. A similar shortening has been observed in a chloro-substituted (*deloc*-2,3,5)-bicyclo[2.1.1]hex-2-en-5-ylium ion.[21]

The gas-phase structure of Me-**1**$^+$ has also been computed on the B3LYP/6-311+G(d,p) level for comparison; see Table S2. The interaction between C9 and the C4a−C8a bond is somewhat stronger in the experimentally determined structure than in the computed structure, as can be seen from the angles between these two bridges: 95.7(6)° vs 98.6°. The aromatic bond lengths show a similar pattern as in the crystal structure; see Figure 4.

Another remarkable feature of Me-**1**$^+$ is the nonplanarity of the aromatic ring. The plane *P*(4a,5,8,8a) is bent upward (i.e., toward the C9 bridge) with regard to *P*(1,4,4a,8a) by 9.6(8)° (see Figure 2 and Table S2), and the plane *P*(5,6,7,8) is bent downward with regard to *P*(4a,5,8,8a) by 5.2(8)°. This leads to the pyramidalizations[22] $\Delta_{C4a} \equiv \Delta_{C8a} = 0.077(5)$ Å. Similar ring

(20) Allen, F. H.; Watson, D. G.; Brammer, L.; Orpen, A. G.; Taylor, R. In *International Tables for Crystallography, Volume C*; Prince, E., Ed.; Kluwer Academic Publishers: Dordrecht, 2004; pp 790−811.
(21) Laube, T.; Lohse, C. *J. Am. Chem. Soc.* **1994**, *116*, 9001−9008.
(22) The pyramidalization is the distance of a trigonal atom from the plane defined by its bond partners.

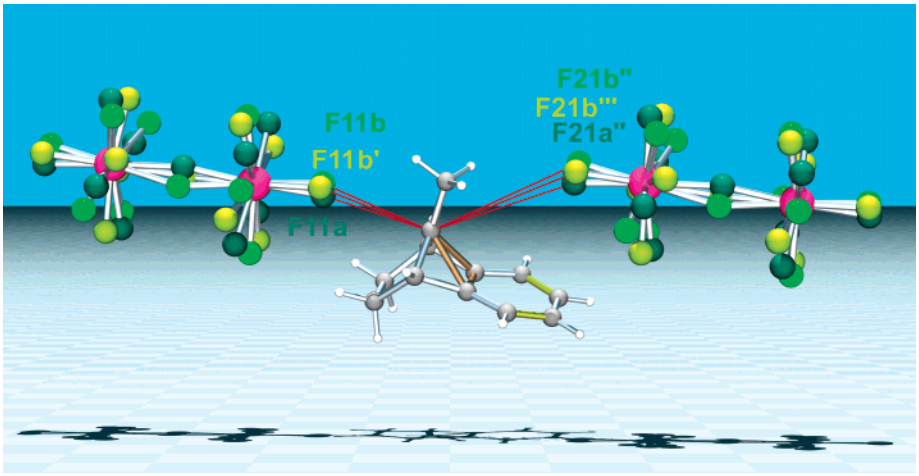

Figure 5. Ball and stick diagram of Me-$\mathbf{1}^+$ and the two anions in the proximity of C9 in the crystal. The symmetry operations are as follows: $' = x, {}^1/_2 - y, z$; $'' = x, y, z + 1$; $''' = x, {}^1/_2 - y, z + 1$. The C9···F contacts are indicated by thin red sticks; for the bond and fluorine colors, see also the legend of Figure 1.

deformations have also been observed in the computed structure of H-$\mathbf{1}^+$.[8] The corresponding deformations of the aromatic ring in the computed structure of **6** have opposite directions and are much weaker.

The packing of the cations and anions (Figure 5) shows a feature seen already in many other carbocation structures:[23] the positively charged carbon atom C9 has on its anti side a close contact with F11 or the corresponding disordered sites F11a, F11b, F11b′ (smallest C9···F, C9···F11a = 3.03(2) Å; sum of the van der Waals radii[24] of C and F, 1.70 Å + 1.47 Å = 3.17 Å). The closest anion contact on the syn side of C9 occurs with F21 of a symmetry-related anion or its disordered sites F21a″, F21b″, F21b‴ (smallest C9···F: C9···F21a″ = 4.12(2) Å), but this is about 1 Å more than the sum of the van der Waals radii. The same F atom is also situated in the proximity of the aromatic C atoms (C4a···F21a″ ≡ C8a···F21a″ = 4.09(2) Å, C5···F21a″ ≡ C8···F21a″ = 3.84(2) Å, C6···F21a″ ≡ C7···F21a″ = 3.65-(2) Å). No anion is found on the other side of the aromatic ring (or on the endo side of the C4a−C8a bond, as in the crystal structure of a substituted norbornenyl cation[25]), but a methyl group of another cation is located in its proximity; see Figure 6. The free space between the anions in the *a* direction illustrates the fact that the anions have rotational degrees of freedom leading to the observed disorder.

The arrangement of anions around a cationic C atom seems to be reasonable for electrostatic reasons, but it can also be interpreted in terms of the reaction coordinate[26] of a nucleophilic attack on C9 leading to anti or syn products, respectively. The close C9···F contact on the anti side of C9 agrees with the observation of Volz et al.[7] that quenching of Me-$\mathbf{1}^+$ with MeOH/MeONa yields only the corresponding anti ether.

In previous papers (ref 9, Figure 7; ref 25, Figure 9), we discussed the possibility that the observed bridged structures in the crystal could be a static or dynamic superposition of classical carbocations. We found that the expected distances between disordered atoms of the hypothetical classical cations were too large to remain undetected in a thermal motion analysis or that the disordered atoms should even have resolvable

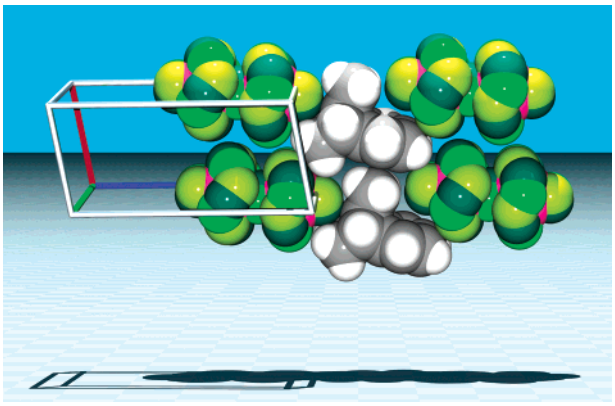

Figure 6. Space-filling diagram showing the surrounding of Me-$\mathbf{1}^+$ in the crystal. The unit cell is shown as parallelepiped (axes: *a*, red; *b*, green; *c*, blue). The arrangement from Figure 5 is drawn twice differing by the translation vector (1,0,0). For the fluorine colors, see also the legend of Figure 1.

positions. This is also the case for Me-$\mathbf{1}^+$ if one uses suitable neutral molecules as models[27] for classical ions. We now also analyze the potential energy surface of the carbocation optimized at a somewhat lower level of theory if compared with its fully optimized structure (see Table S2). The potential energy surface (Figure 7; the conformation of the cation in the crystal lies 0.6 kcal/mol above the minimum of the depicted function) shows only one minimum for the bridged structure. The potential energy function is not symmetrical along the diagonal (C4a−C9 = C8a−C9) indicating that weakening the (3c, 2e) bond is easier than strengthening it. There is no hint that classical isomers, which should have C4a−C9 ≈ 1.63 Å and C8a···C9 ≈ 2.09 Å (or vice versa), are stable species. They are expected to be ∼9 kcal/mol higher in energy if compared with the bridged structure.

The structure of $\mathbf{5}^+$ in the crystal is shown in Figures 8 and 9. The most remarkable feature is the fact that the carbon skeleton of this ion is structurally more similar to the hydrocarbon **6** or to its precursor **18**[27] than to a bridged cation like Me-$\mathbf{1}^+$. The angle between the C9 bridge and the C4a,C8a bridge is 122.38(10)° if compared with 126.1° for **6** and 95.7(6)° for Me-$\mathbf{1}^+$. The C−O bond length (1.480(2) Å) is elongated

(23) Laube, T. *Chem. Rev.* **1998**, *98*, 1277−1312.
(24) Bondi, A. *J. Phys. Chem.* **1964**, *68*, 441−451.
(25) Laube, T. *J. Am. Chem. Soc.* **1989**, *111*, 9224−9232.
(26) Bürgi, H. B.; Dunitz, J. D. *Acc. Chem. Res.* **1983**, *16*, 153−161.

(27) DFT results are given in the Supporting Information.

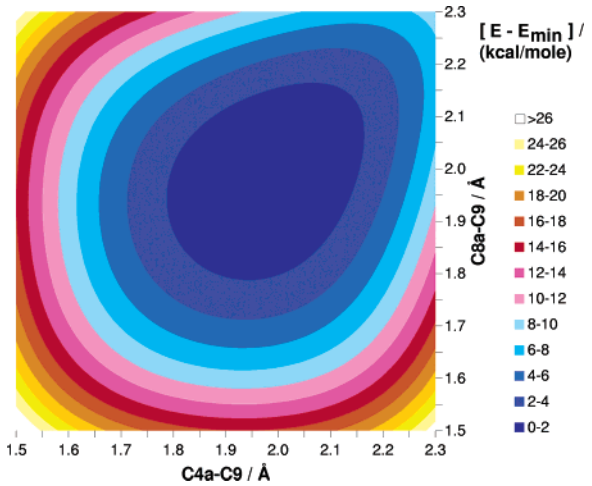

Figure 7. Contour line diagram of the calculated potential energy surface of Me-**1**$^+$ in the gas phase depending on the lengths of the weak bonds (C4a−C9 and C8a−C9) of the assumed (3c, 2e) bond involving C4a, C8a, C9. The potential energies were computed by optimizing the structure at the B3LYP/6-311++G(3df,3pd)// B3LYP/6-31G(d) level with the constraints C4a−C9 = 1.5(0.2)2.3 Å and C8a−C9 = 1.5(0.2)2.3 Å (relaxed potential energy surface scan). The plotted function is a least-squares 4th order polynomial in two variables, which is symmetrical with regard to an exchange of the independent variables. E_{min} is the energy at the minimum of the adjusted polynomial.

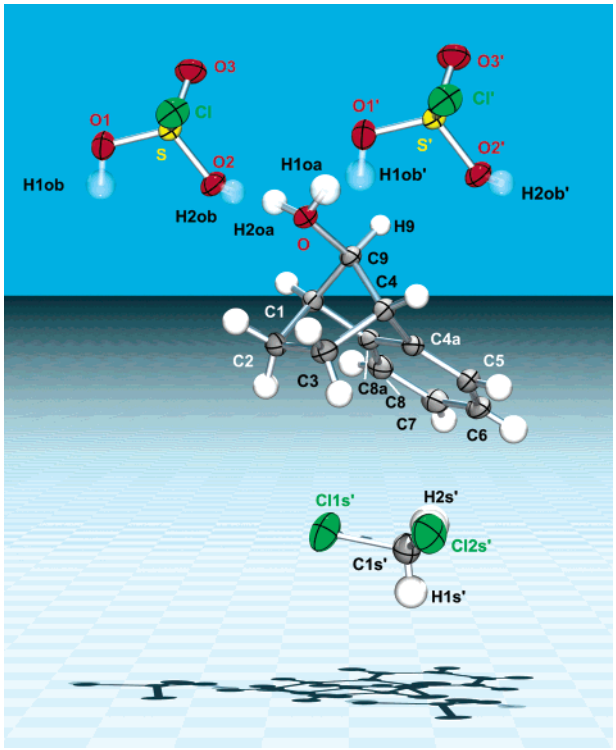

Figure 8. ORTEP representation of the crystal structure of **5**$^+$ $SO_3Cl^-\cdot CH_2Cl_2$. The additional anion is shown to depict the hydrogen bonds. Two sites are drawn for each of the disordered oxonium H atoms (H1o and H2o): the major oxonium H sites (H1oa, sof = 0.76(4); H2oa, sof = 0.71(4)) are drawn as weakly transparent spheres, and the corresponding minor sites (H1ob, H2ob), as more transparent spheres. The symmetry-related atoms have primed labels ($'$ = x, y − 1, z). The displacement ellipsoids and the hydrogen spheres are drawn at the 50% probability level.

by 0.048(2) Å if compared with the average C−O bond length in secondary alcohols (1.432(1) Å).[20] A similar C−O elongation upon protonation (0.04(1) Å) is observed in the crystal structure of $MeOH_2^+$ (C−O = 1.45(1) Å)[28] if compared with MeOH in

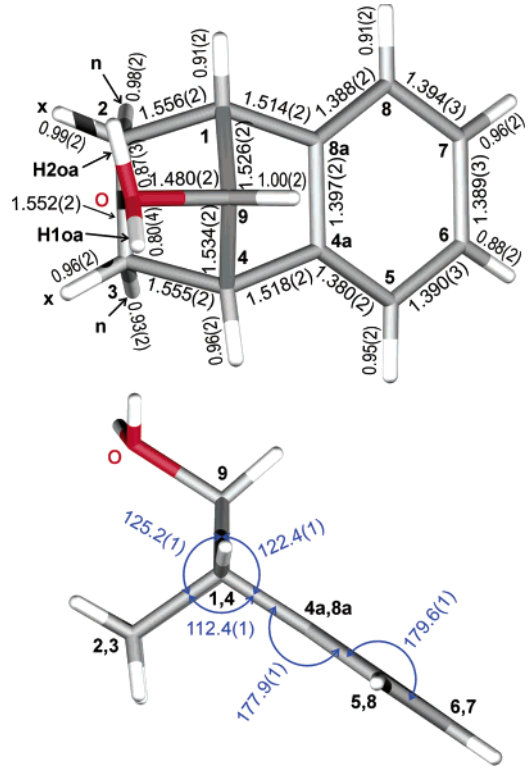

Figure 9. Geometry of the cation in the crystal structure of **5**$^+$ $SO_3Cl^-\cdot CH_2Cl_2$ (Distances in Å. Blue: interplanar angles in deg). The hydrogen atom numbers (not drawn) correspond to their carbon atoms (x = exo, n = endo). Bottom: approximate Newman projection along C1−C4.

crystal structures (C−O = 1.413(5) Å).[20] The observed C−O bond in **5**$^+$ is not as long as the C−O bonds in the computed structures of protonated *tert*-BuOH (C−O = 1.663 Å)[29] or of protonated 2-norbornanols ($C-O_{exo}$ = 1.624 Å; $C-O_{endo}$ = 1.615 Å)[30] or of other protonated alcohols.[31] The results of Uggerud et al.[31] show that the C−O bonds of protonated alcohols become shorter upon complexation with a water molecule (*i*-$PrOH_2^+$, C−O = 1.579 Å; *i*-$PrOH_2^+\cdot OH_2$, C−O = 1.532 Å).[32] Therefore we computed also the structure of **5**$^+$ in the gas phase and in water[33] (Table S2). The experimental structure of **5**$^+$ is more similar to the computed structure of **5**$^+$ in water (C−O = 1.526 Å) than in the gas phase (C−O = 1.704 Å). The unusual C−O bond length in the computed gas-phase structure of **5**$^+$ made an investigation of its potential energy surface necessary: the potential energy as a function of C4a−C9 = C8a−C9 is shown in Figure 10.

One sees a double-minimum system, where **5**$^+$ is about 1.5 kcal/mol higher in energy if compared with the absolute

(28) Minkwitz, R.; Schneider, S. *Z. Anorg. Allg. Chem.* **1998**, *624*, 1989−1993.
(29) Jorgensen, W. L.; Buckner, J. K.; Huston, S. E.; Rossky, P. J. *J. Am. Chem. Soc.* **1987**, *109*, 1891−1899.
(30) Schreiner, P. R.; Schleyer, P. v. R.; Schaefer, H. F., III. *J. Org. Chem.* **1997**, *62*, 4216−4228.
(31) Uggerud, E.; Bache-Andreassen, L. *Chem.—Eur. J.* **1999**, *5*, 1917−1930.
(32) A probably related shortening of a B−N bond is observed in H_3B-NH_3. (a) Bühl, M.; Steinke, T.; Schleyer, P. v. R.; Boese, R. *Angew. Chem., Int. Ed. Engl.* **1991**, *30*, 1160−1161. (b) Dillen, J.; Verhoeven, P. *J. Phys. Chem. A* **2003**, *107*, 2570−2577. (c) Leopold, K. R.; Canagaratna, M.; Phillips, J. A. *Acc. Chem. Res.* **1997**, *30*, 57−64.
(33) We choose water as solvent because it is the solvent with the highest dielectric constant for which predefined parameters are available, see computational section. We assume that the environment of **5**$^+$ in the crystal is also very polar due to the cation−anion contacts. The dielectric constant of $ClSO_3H$ is 60 ± 10 at 15° C according to: Cremlyn, R. J. *Chlorosulfonic Acid*; Royal Society of Chemistry: Cambridge, 2002; p 2.

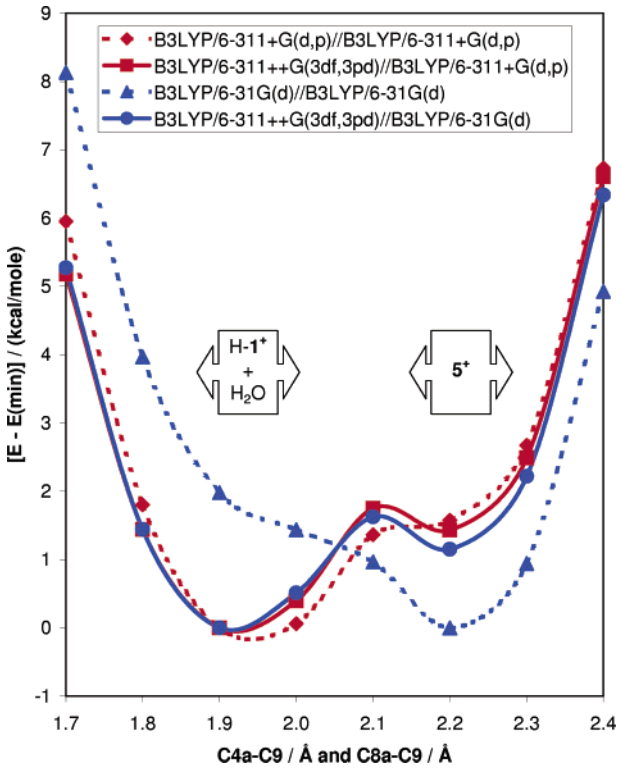

Figure 10. Potential energy of $\mathbf{5}^+$ and of the water complex of H-$\mathbf{1}^+$ in the gas phase calculated at various levels of theory as a function of the bond length C4a−C9 = C8a−C9. The abscissa can be seen as the reaction coordinate of the approach of the C9 bridge toward the C4a−C8a bond retaining $m = C_s$ symmetry. The structures of the conformations were optimized with the constraints C4a−C9 = C8a−C9 = 1.7(0.1)2.4 Å. The plotted functions are interpolants. Blue: lower level geometry. Red: higher level geometry. Solid functions represent energies computed at a higher level of theory if compared with the dashed ones. The boxes with arrows indicate qualitatively the ranges of existence of the various ions.

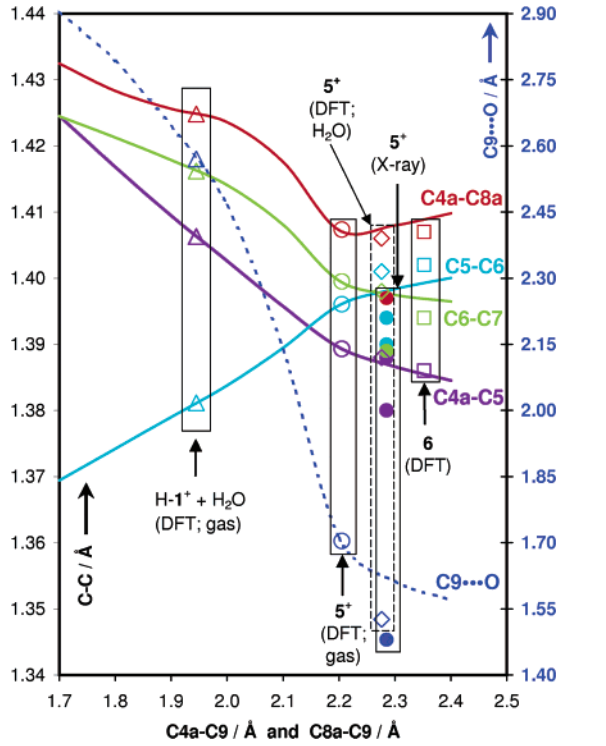

Figure 11. Computed benzene ring C−C bond lengths (solid lines; left scale) and C9−O bond length (dashed line; right scale) of $\mathbf{5}^+$ in the gas phase as functions of the bond length C4a−C9 = C8a−C9. The abscissa can be seen as the reaction coordinate of the approach of the C9 bridge toward the C4a−C8a bond retaining $m = C_s$ symmetry. The structures of the conformations were optimized at the B3LYP/6-311+G(d,p) level with the constraints C4a−C9 = C8a−C9 = 1.7(0.1)2.4 Å (relaxed potential energy surface scan). The plotted functions are interpolants. The bond lengths of the crystal structure are drawn as filled circles, and those of various computed structures as empty symbols with the corresponding color (data: see Table S2 and Supporting Information).

minimum, a H-$\mathbf{1}^+$/water complex.[34] In Figure 11 various bond lengths of the experimental structure of $\mathbf{5}^+$ and of some computed structures are drawn along the reaction coordinate of the bridging. Based on the C−O and on the C4a−C9 = C8a−C9 bond lengths, one can say that there is only a very weak interaction or bridging between the π system and C9 in the crystal; i.e., the experimental structure of $\mathbf{5}^+$ must be seen as an early point on the reaction coordinate of the dissociation into H-$\mathbf{1}^+$ and H_2O.

The crystal packing (Figure 12) shows infinite chains consisting of cations and anions in alternating order, which are connected via H bonds in the *b* direction. The geometrical parameters (O···O ≈ 2.55 Å; see Figure 13) indicate that the H bonds are strong.[35] The interaction between O and O3″ may be interpreted as an additional bifurcated H bond.[36,37] The chlorosulfonate anion in our structure is not significantly different from the anion in NO^+ SO_3Cl^- reported Höhle and Mijlhoff[38] (the only other crystal structure in the literature containing a chlorosulfonate anion). There is a significant shortening of the S−Cl bond (2.0506(6) Å) if compared with the structure computed by Steudel et al. in the gas phase[39] (S−Cl = 2.242 Å).[40] Each CH_2Cl_2 molecule is interacting with another CH_2Cl_2 molecule and the Cl atom of an anion in a very characteristic angle pattern (Figure 14).

These Cl···Cl interactions are also observed in the crystal structures of CH_2Cl_2[41] (Cl···Cl = 3.492 Å) and of Cl_2[42] (Cl···Cl = 3.258 Å). They may be interpreted as nucleophile−electrophile interactions as suggested by Bent;[43] i.e., the CH_2Cl_2 molecule is not simply situated in a cavity of suitable size.

Several details of the structure of $\mathbf{5}^+$ $SO_3Cl^-\cdot CH_2Cl_2$ attract attention. The site occupation factors (sof) of the H atoms on the oxonium O atom (H1oa, H2oa) are significantly smaller than 1 if they are refined. If we assume that this is not an artifact resulting from the usual difficulties in refining H atoms in X-ray crystal structures, the missing H atom populations can be refined with geometrical and U_{iso} constraints on the anion O atoms closest to the major H sites: O1 and O2 (H1ob and H2ob).

(34) It was obviously a fortunate coincidence that the optimization on the B3LYP/6-311+G(d,p) level lead to the local minimum $\mathbf{5}^+$. The barrier between $\mathbf{5}^+$ and the H-$\mathbf{1}^+$/water complex increases only with the large basis set; see Figure 10.
(35) Jeffrey, G. A. *An Introduction to Hydrogen Bonding*; Oxford University Press: Oxford, 1997; pp 33−55.
(36) Taylor, R.; Kennard, O.; Versichel, W. *J. Am. Chem. Soc.* **1984**, *106*, 244−248. Rozas, I.; Alkorta, I.; Elguero, J. *J. Phys. Chem. A* **1998**, *102*, 9925−9932.
(37) A similar H bond network is observed in the crystal structure of $MeOH_2^+$ AsF_6^-.[28]
(38) Höhle, T.; Mijlhoff, F. C. *Recl. Trav. Chim. Pays-Bas* **1967**, *86*, 1153−1158.
(39) Steudel, R.; Otto, A. H. *Eur. J. Inorg. Chem.* **2000**, 2379−2386.
(40) S−Cl bond lengths computed by the B3LYP/6-311+G(d,p) method in the gas phase: SO_3Cl^- 2.290 Å; **18**·$ClSO_3H$ 2.108 Å. See Supporting Information.
(41) Kawaguchi, T.; Tanaka, K.; Takeuchi, T.; Watanabé, T. *Bull. Chem. Soc. Jpn.* **1973**, *46*, 62−66.
(42) Powell, B. M.; Heal, K. M.; Torrie, B. H. *Mol. Phys.* **1984**, *53*, 929−939.
(43) Bent, H. A. *Chem. Rev.* **1968**, *68*, 587−648.

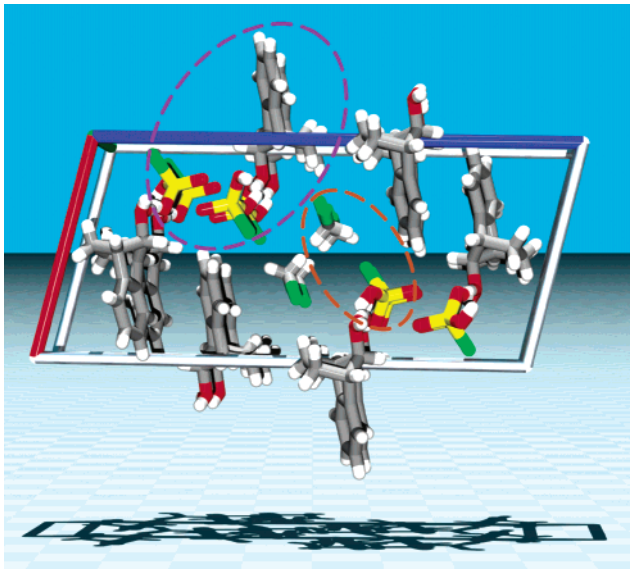

Figure 12. Crystal packing of 5^+ $SO_3Cl^-\cdot CH_2Cl_2$. The unit cell is shown as parallelepiped (axes: *a*, red; *b*, green; *c*, blue). The interactions in chains along the *b* axis consisting of cations and anions (violet ellipse) and in chains consisting of anions and CH_2Cl_2 molecules (orange ellipse) are depicted in Figures 13 and 14.

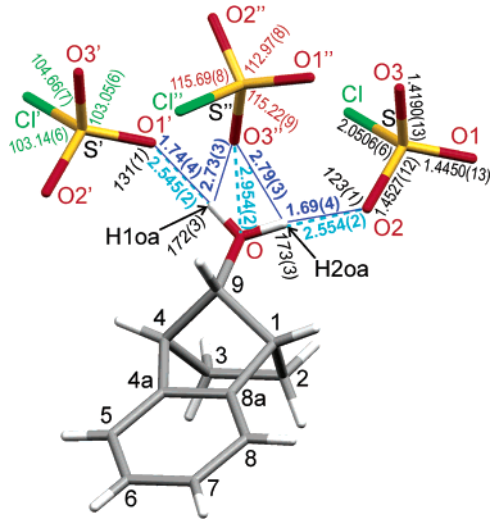

Figure 13. Geometry of the H bonds and of the anion in the crystal structure of 5^+ $SO_3Cl^-\cdot CH_2Cl_2$ (symmetry operations: $' = x, y - 1, z$; $'' = -x + {}^1/_2, y - {}^1/_2, -z + {}^1/_2$; see also Figure 12). The H bonds are described by the following parameters: dashed light blue lines = O···O distances, solid dark blue lines = H···O distances, italic = O−H···O and H···O−S angles. Only the major H sites are drawn. Anion: red = O−S−O angles, green = Cl−S−O angles.

This would mean that the measured crystal structure is an averaged or disordered structure consisting of superimposed cations $\mathbf{5}^+$ and alcohol molecules **18** on the cation site, and of superimposed SO_3Cl^- anions and $ClSO_3H$ molecules on the anion site. While H bond disorder is well-known for certain forms of ice and other structures,[44−47] it is more difficult to understand in the structure of 5^+ $SO_3Cl^-\cdot CH_2Cl_2$. The estimated

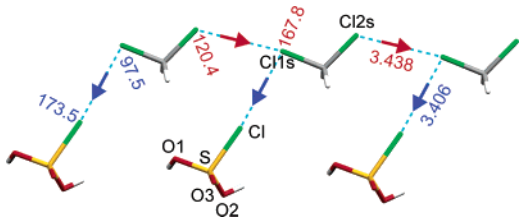

Figure 14. Geometry of the Cl···Cl interactions in the crystal structure of 5^+ $SO_3Cl^-\cdot CH_2Cl_2$ (symmetry operations omitted for clarity). The three anions (drawn with the minor hydrogen sites) and the three CH_2Cl_2 molecules are symmetry-related by the translation vector (0,1,0), see Figure 12. Dashed light blue lines mark the contacts, the arrows point from the nucleophilic to the electrophilic atom. Red: solvent−solvent interactions; blue: solvent-anion interactions.

pK_a for protonated secondary alcohols relative to water in the condensed phase is about −2.[48] An estimated pK_a value for chlorosulfonic acid of −6 is reported by Guthrie,[49] and from the Hammett acidity function H_0[50] it could be cautiously estimated that the pK_a lies around the range from −9 (approximate pK_a for H_2SO_4)[48a] to −12 (approximate pK_a for FSO_3H).[48a] Such a pK_a difference should guarantee a practically complete protonation of the alcohol. On the other hand, DFT calculations of the energy profile of the proton transfer in an isolated ion pair constrained to a geometry as in the asymmetric unit of the crystal structure indicates that the proton is completely transferred to the anion; i.e., a molecular complex **18**·$ClSO_3H$ is present (see Figure 15).

A second minimum describing an ion pair $\mathbf{5}^+$ SO_3Cl^- does not exist; only a shoulder is recognizable. We optimized also the structure of an unconstrained ion pair and obtained also only a hydrogen-bonded complex **18**·$ClSO_3H$.[27] These results show that an isolated ion pair in the gas phase is not a suitable model for $\mathbf{5}^+$ SO_3Cl^- in the crystal. In view of the discrepancy between the pK_a value prediction ($\mathbf{5}^+$ SO_3Cl^- much more stable) and the gas-phase DFT calculations (**18**·$ClSO_3H$ much more stable), we assume that the experimentally observed energetic similarity of the two sites of each oxonium proton is the result of a cooperative effect in the infinite cation−anion chains in the crystal.

The SO_3Cl^- anion does not have local $3m = C_{3v}$ symmetry. The O_{anion} atoms engaged in the strong H bonds (O1 and O2) have longer S−O bonds and smaller Cl−S−O angles than O3, and O1−S−O2 is smaller than the other O−S−O angles (Figure 13); i.e., the anion has only approximate $m = C_s$ symmetry with the mirror plane passing through O3, S, and Cl. Such structural deviations are usually ascribed to packing interactions, but in this case they could at least partially be the result of an averaging of $ClSO_3H$ and SO_3Cl^- structures due to the unresolved disorder mentioned above. Therefore the structural parameters of $\mathbf{5}^+$ in the crystal must be interpreted carefully. The observed C9−O

(44) Structure of ice I_h: Leadbetter, A. J.; Ward, R. C.; Clark, J. W.; Tucker, P. A.; Matsuo, T.; Suga, H. *J. Chem. Phys.* **1985**, *82*, 424−428.
(45) Structure of malonaldehyde: Rowe, W. F., Jr.; Duerst, R. W.; Wilson, E. B. *J. Am. Chem. Soc.* **1976**, *98*, 4021−4023. Perrin, C. L.; Thoburn, J. D. *J. Am. Chem. Soc.* **1989**, *111*, 8010−8012.
(46) Proton transfer in acid base complexes: Lethonen, O.; Hartikainen, J.; Rissanen, K.; Ikkala, O.; Pietilä, L.-O. *J. Chem. Phys.* **2002**, *116*, 2417−2424. Chipot, C.; Gorb, L. G.; Rivail, J.-L. *J. Phys. Chem.* **1994**, *98*, 1601−1607.
(47) Selected papers about double minimum hydrogen bonds: Novak, A. *Struct. Bonding (Berlin)* **1974**, *18*, 177−216. Bernstein, J.; Etter, M. C.; Leiserowitz, L. The Role of Hydrogen Bonding in Molecular Assemblies. In *Structure Correlation, Volume 2*; Bürgi, H.-B., Dunitz, J. D., Eds.; VCH: Weinheim, 1994; pp 431−507.
(48) (a) Smith, M. B.; March, J. *March's Advanced Organic Chemistry*, 5th ed.; Wiley: New York, 2001; pp 329−331. (b) Literature values of the pK_a of 2-propanol between −0.35 and −5.2 (depending on the analytical method) are reported in: Arnett, E. M.; Quirk, R. P.; Burke, J. J. *J. Am. Chem. Soc.* **1970**, *92*, 1260−1266.
(49) Guthrie, J. P. *Can. J. Chem.* **1978**, *56*, 2342−2354.
(50) $H_0(ClSO_3H) = -13.80$: Gillespie, R. J.; Peel, T. E.; Robinson, E. A. *J. Am. Chem. Soc.* **1971**, *93*, 5083−5087. $H_0(H_2SO_4) = -11.93$, $H_0(FSO_3H) = -15.07$: Gillespie, R. J.; Peel, T. E. *J. Am. Chem. Soc.* **1973**, *95*, 5173−5178.

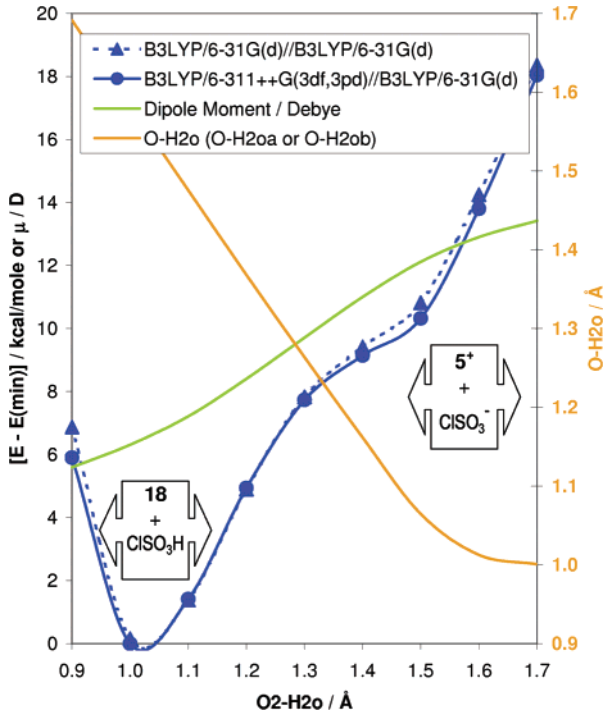

Figure 15. Potential energy of an ion pair $\mathbf{5}^+$ $ClSO_3^-$ and of the molecular complex **18**·$ClSO_3H$ in the gas phase calculated at various levels of theory as function of the bond length O2−H2o (blue functions). The abscissa can be seen as the reaction coordinate of the proton transfer. The structures of the conformations were optimized with several constraints to retain a mutual spatial orientation of the ions or molecules as found in the asymmetric unit of the crystal structure (see Supporting Information). The dipole moment (green) increases upon formation of the ion pair. The distance O−H2o (orange) is a nearly linear function of O2−H2o up to O2−H2o ≈ 1.55 Å because O2−H2o−O ≥ 160°. The boxes with arrows indicate qualitatively the ranges of existence of the various complexes.

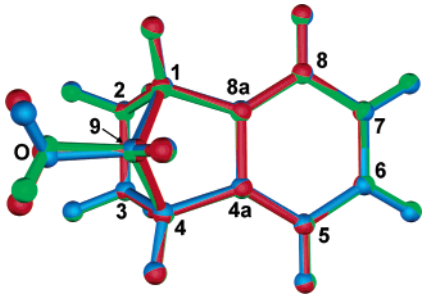

Figure 16. Superposition of $\mathbf{5}^+$ (DFT, water; red) on the two enantiomers of **18** (DFT, gas phase; green and blue). The slight asymmetry is the result of the least squares adjustment (only heavy atoms) of $\mathbf{5}^+$ on a weighted average of **18** and *ent*-**18** (the weights were derived from the sofs).

bond length (1.480(2) Å) could be seen as a lower boundary for its true value. Assuming the correctness of the H site occupation factors, the structure is a superposition of 47(5)% $\mathbf{5}^+$ and of 53(5)% **18** (24% of one and 29% of the other enantiomeric conformers). A simple superposition of $\mathbf{5}^+$ (DFT, H_2O) and **18** (DFT, gas phase) shows that such a disorder would be impossible to detect by investigation of the atomic displacement ellipsoids because of the very similar structures (see Figure 16).

The weighted average of the C−O bond lengths of $\mathbf{5}^+$ (DFT, H_2O 1.526 Å; see Table S2) and of **18** (DFT, gas phase 1.420 Å) is 1.469 Å and thus in sufficient agreement with the observed value.[51] The C−O elongation upon protonation in our structure (0.048(2) Å) is comparable to the corresponding elongation in

Chart 2. Interpretation of the Structure of Me-$\mathbf{1}^+$

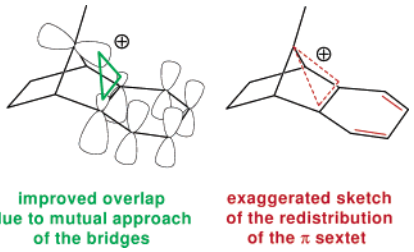

the $MeOH_2^+$ structure (0.04(1) Å),[28] for which a proton disorder is not expected due to the weakly coordinating AsF_6^- anion. One would expect a significantly larger C−O elongation for $\mathbf{5}^+$ because it is probably the precursor[52] of the short-lived carbocation H-$\mathbf{1}^+$ and could advance on the reaction coordinate of the H_2O elimination, whereas $MeOH_2^+$ is not a cation precursor, although $MeOH_2^+$ could loose H_2O in an S_N2 reaction. Thus the similar estimated C−O bond elongations upon protonation also support our $\mathbf{5}^+$/**18** disorder hypothesis.[53] Olah et al.[54] observed in NMR experiments a decomposition temperature of $MeOH_2^+$ around +50° C, whereas other protonated alcohols decompose at a much lower temperature; this demonstrates the higher stability of $MeOH_2^+$. Additional support for the disorder hypothesis of $\mathbf{5}^+$ may be seen in the similarity between the crystal structures of $\mathbf{5}^+$ and of the rather stable, neutral **2** (X = brosylate).[55] Comparing these two potential precursors of H-$\mathbf{1}^+$, one would expect $\mathbf{5}^+$ to be more advanced on the reaction coordinate toward H-$\mathbf{1}^+$, because the brosylate dissociation involves a charge separation.[56] Unfortunately the problem of this kind of potential disorder has not been discussed in related crystal structures containing H_2SO_4 or FSO_3H (see Supporting Information).

Shin et al.[6a] assumed that they observed $\mathbf{5}^+$ in two different superacidic media by ^1H NMR spectroscopy. We recorded the ^1H NMR spectrum of a mixture of **18** with an excess of $ClSO_3H$ in CD_2Cl_2 and obtained a spectrum similar to the spectrum in FSO_3H/SO_2ClF reported by Shin et al.. GIAO calculations of $\mathbf{5}^+$ SO_3Cl^- and **18**·$ClSO_3H$ (crystal geometry or fully optimized) at the B3LYP/6-311++G(2d,2p) level[27] show a better agreement with our experimental chemical shifts than those of free $\mathbf{5}^+$. We cannot decide on the basis of the GIAO calculations whether complexes containing $\mathbf{5}^+$ or **18** or mixtures of them are present in a $ClSO_3H/CD_2Cl_2$ solution.

Conclusion

The crystal structure of Me-$\mathbf{1}^+$ can be interpreted as shown in Chart 2. The π electron cloud is partially delocalized into the empty p orbital at C9. This leads to a mutual approach of the C9 and the C4a−C8a bridges. From the bond lengths in

(51) Semiempirical calculations (MOPAC, AM1) yield the following C−O bond lengths: $\mathbf{5}^+$ 1.512 Å, **18** 1.406 Å.
(52) We do not have any experimental information that $\mathbf{5}^+$ is a precursor of H-$\mathbf{1}^+$. The energy profile depicted in Figure 10 shows that this reaction may easily take place in the gas phase.
(53) The C−O bond length in the $MeOH_2^+$ crystal structure may be influenced by weak C···F contacts anti to the C−O bond, which could advance the cation somewhat towards a S_N2 transition state.
(54) Olah, G. A.; Sommer, J.; Namanworth, E. *J. Am. Chem. Soc.* **1967**, *89*, 3576−3581.
(55) Koyama, H.; Okada, K. *J. Chem. Soc. B* **1969**, 940−950.
(56) If one compares the crystal structures of benzonorbornenes with 9-syn and 9-anti leaving groups, the 9-anti derivatives have slightly shorter C4a−C9 and C8a−C9 contacts than the 9-syn derivatives. See Supporting Information.

the benzene-like ring, we conclude that a (3c, 2e) bond interacting with a butadienyl system is a suitable description of Me-**1**$^+$ as suggested by Bartlett et al..[2] The experimentally determined structure shows a higher degree of bridging than the computed DFT gas-phase structure.

The crystal structure of **5**$^+$ is probably disordered with **18** and can thus only cautiously be interpreted. The C skeleton indicates only a weak interaction between the C9 and the C4a−C8a bridges. The observed elongation of the C−O bond upon protonation is 0.048(2) Å or more. DFT calculations of **5**$^+$ in the gas phase are not appropriate for a description in the crystal because of the high tendency to dissociate into a H-**1**$^+$/water complex observed in the calculations. If the polar environment of **5**$^+$ in the crystal is simulated by a DFT calculation in water, a relatively good description with the exception of the C−O bond length is achieved. With regard to the C−O bond length, the ion **5**$^+$ seems to be related to H_3B-NH_3 and other "partially bonded" molecules.[32c] The disordered oxonium proton positions cannot be explained by DFT calculations on isolated ion pairs in the gas phase, which lead to a practically complete proton transfer to the anion, i.e., the hydrogen-bonded complex **18**·$ClSO_3H$. Therefore we assume that the observed equilibrium between the oxonium ion **5**$^+$ and the alcohol **18** in the crystal occurs due to cooperative hydrogen bonds and cation−anion interactions in the infinite chains.

Computational Section

The X-ray data reductions were carried out with teXsan,[57] the absorption corrections (based on multiscans from symmetry-related measurements) were carried out with Sortav.[58] The crystal structures were solved with SHELXS[59] and refined with SHELXL.[60] Analyses of the refined structures were carried out with PLATON[61] and analyses of the reciprocal space data have been displayed also with FOTOPLOT.[62] Experimental reference structures have been retrieved from the Cambridge Structural Database.[63] Semiempirical calculations were carried out with SYBYL 6.0[64]/MOPAC,[65] DFT calculations with Gaussian 03 W[66] with GaussView 3.09.[67] Molecular modeling was carried out with SYBYL 6.0[64] and ViewerPro.[68] ADP, ball-and-stick, and packing diagrams were produced with Ortep.[69,70] Photorealistic graphics were generated with POV-Ray.[71]

Acknowledgment. We thank Dr. Anthony Linden (University of Zurich, Zurich, Switzerland) for carrying out the X-ray measurements and Mrs. Sandra Weber (Cilag AG) for help with the syntheses.

Supporting Information Available: Tables S1 and S2, Experimental Section. Tables and additional graphics of the crystal structure data, NMR spectra, results of quantum chemical calculations, data about various structures from the literature mentioned in the discussion. Two X-ray crystallographic files in CIF format. This material is available free of charge via the Internet at http://pubs.acs.org.

JA040115T

(57) *teXsan* 1.10 (Unix version); Molecular Structure Corporation: The Woodlands, TX.
(58) Blessing, R. H. *Acta Crystallogr., Sect. A* **1995**, *A51*, 33−38.
(59) Sheldrick, G. M. *SHELXS-97 − CRYSTAL STRUCTURE SOLUTION − UNIX VERSION*, release 97-2; University of Göttingen: Göttingen, Germany, 1997.
(60) Sheldrick, G. M. *SHELXL-97 − CRYSTAL STRUCTURE REFINEMENT − UNIX VERSION*, release 97-2; University of Göttingen: Göttingen, Germany, 1997.
(61) Spek, A. L. *PLATON: A Multipurpose Crystallographic Tool*; Utrecht University: Utrecht, The Netherlands, 2002. Farrugia, L. J. *Platon for Windows*; University of Glasgow: Glasgow, U.K., 2002.
(62) Laube, T. *FOTOPLOT*, version 6; Schaffhausen, Switzerland, 2001.
(63) Allen, F. H. *Acta Crystallogr., Sect. B* **2002**, *B58*, 380−388. Bruno, I. J.; Cole, J. C.; Edgington, P. R.; Kessler, M. K.; Macrae, C. F.; McCabe, P.; Pearson J.; Taylor, R. *Acta Crystallogr., Sect. B* **2002**, *B58*, 389−397.
(64) *SYBYL 6.0*; Tripos Inc.: St. Louis, MO, 1992.
(65) Stewart, J. J. P. *MOPAC*, version 5.0 (integrated in *SYBYL 6.0*[64]); QCPE #455.
(66) Frisch, M. J.; Trucks, G. W.; Schlegel, H. B.; Scuseria, G. E.; Robb, M. A.; Cheeseman, J. R.; Montgomery, J. A., Jr.; Vreven, T.; Kudin, K. N.; Burant, J. C.; Millam, J. M.; Iyengar, S. S.; Tomasi, J.; Barone, V.; Mennucci, B.; Cossi, M.; Scalmani, G.; Rega, N.; Petersson, G. A.; Nakatsuji, H.; Hada, M.; Ehara, M.; Toyota, K.; Fukuda, R.; Hasegawa, J.; Ishida, M.; Nakajima, T.; Honda, Y.; Kitao, O.; Nakai, H.; Klene, M.; Li, X.; Knox, J. E.; Hratchian, H. P.; Cross, J. B.; Adamo, C.; Jaramillo, J.; Gomperts, R.; Stratmann, R. E.; Yazyev, O.; Austin, A. J.; Cammi, R.; Pomelli, C.; Ochterski, J. W.; Ayala, P. Y.; Morokuma, K.; Voth, G. A.; Salvador, P.; Dannenberg, J. J.; Zakrzewski, V. G.; Dapprich, S.; Daniels, A. D.; Strain, M. C.; Farkas, O.; Malick, D. K.; Rabuck, A. D.; Raghavachari, K.; Foresman, J. B.; Ortiz, J. V.; Cui, Q.; Baboul, A. G.; Clifford, S.; Cioslowski, J.; Stefanov, B. B.; Liu, G.; Liashenko, A.; Piskorz, P.; Komaromi, I.; Martin, R. L.; Fox, D. J.; Keith, T.; Al-Laham, M. A.; Peng, C. Y.; Nanayakkara, A.; Challacombe, M.; Gill, P. M. W.; Johnson, B.; Chen, W.; Wong, M. W.; Gonzalez, C.; Pople, J. A. *Gaussian 03W*, revision B.03; Gaussian, Inc.: Pittsburgh, PA, 2003.
(67) *GaussView 3.09*; Gaussian, Inc.: Pittsburgh, PA, 2003.
(68) *Discovery Studio ViewerPro*; Accelrys Inc.: San Diego, CA, 2002.
(69) Burnett, M. N.; Johnson, C. K. *ORTEP-III*: *Oak Ridge Thermal Ellipsoid Plot Program for Crystal Structure Illustrations*; Oak Ridge National Laboratory Report ORNL-6895, 1996.
(70) Farrugia, L. J. *Ortep-3 for Windows version 1.07*; University of Glasgow: Glasgow, U.K., 2001.
(71) POV-Team *POV-Ray*, version 3.1g; c/o Hallam Oaks P/L: P.O. Box 407, Williamstown, Victoria 3016, Australia, 1999.